Proceedings of the
2007 IEEE Intelligent Vehicles Symposium
Istanbul, Turkey, June 13-15, 2007

An Approach to Integrate Vehicle Dynamics in Motion Planning for Advanced Driver Assistance Systems

Tobias Hesse and Thomas Sattel

Abstract— **Path planning procedures belong to the key software elements for advanced driver assistance systems including vehicle following, lane-keeping, lane-changing, or collision avoidance. One approach to realize an integrated driver assistance on the guidance level is based on an elastic band immersed in a potential field hazard map. This paper presents an extension of this elastic band path planning method, incorporating the vehicle dynamics in the elastic band. It is shown that this measure enhances the drivability of the planned paths.**

I. INTRODUCTION

In the near future, drivers will more and more share vehicle guidance with assistance systems. For these advanced driver assistance systems, path planning modules are among the key software modules.

To date, various path planning and motion planning approaches have been proposed for automotive applications, depending on the type of maneuver for which they are provided. For example in [1] a behavior-based approach for autonomous driving is chosen. Therein, the trajectories to execute a lane-change maneuver are computed from a linear bicycle model. Likewise, in [2] a behavior-based approach is developed. However, the trajectories are generated by applying geometric path planning with simple functions like sinusoids. An advanced geometric path planning concept is proposed in [3], for example. Along the corridor in front of the host-vehicle points are fixed, which fulfill the geometric constraints. Two-dimensional splines of the order five interpolate between neighboring points. By using the Bezier-method the course can be locally adapted to sudden changes in the environment. For collision-avoidance maneuvers, [4] uses a kinematic path planning. The trajectory for evasion maneuvers follows from the kinematic relation between the lateral acceleration and the curvature and the assumption of a sinusoid variation of the lateral acceleration. The path planner in [5] generates possible paths from a smoothed version of a given base trajectory, but with varying lateral offsets to avoid collisions with static obstacles. The lateral offsets are computed from a bicycle model. To select the best path, constraints like the imposed corridor or the number of obstacles under the path are evaluated.

Another choice to address path planning tasks are potential field methods. In robotics, potential field based methods for motion planning, introduced by [6] and [7], are well established, see for example [8]. In [9], and in [10] a potential field based path planning approach using elastic bands is proposed. The advantage of this path planning approach among other approaches like geometric path planning is, that traffic objects directly influence the path planning in a temporally and spatially predictive manner. It includes the extrapolated motion of traffic objects in the path planning and does not restrict the planned path to a certain geometric function. However, a measure of drivability, that contributes in shaping the path is not included yet.

To rid the method of this shortcoming, an additional internal potential is introduced within the potential field framework of the elastic band method. This potential influences the path to minimize the predicted tire forces that would be necessary to follow the path. After an overview over the existing method of elastic bands, in a first step the (inverse) vehicle dynamics are analyzed for a given path to determine the expected necessary forces at the tires. Then an additional internal potential V^{dyn} is defined and integrated in the method of elastic bands, to plan a drivable path based on the previously mentioned analysis of the inverse dynamics. Finally, simulation results are presented.

II. ELASTIC BAND PATH PLANNING

The method of elastic bands is a potential field method for collision-free path planning in the presence of obstacles, hazards and obstructions, see [10]. The elastic band is comprised of discrete nodes that are interlinked with springs as shown in Fig. 1. It represents the planned path for the vehicle. The velocity is controlled by the driver. The vehicle's velocity is extrapolated assuming a constant acceleration based on the current driver input. This information is included in the path planning for example with regards to the extrapolated positions of the obstacles.

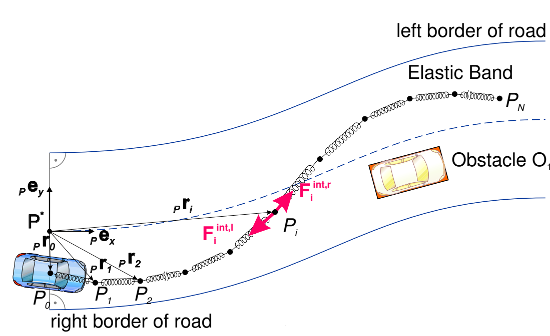

Fig. 1. Concept of elastic bands

This work was supported by the International Graduate School of Dynamic Intelligent Systems

T. Hesse is with the L-LAB and Faculty of Mechanical Engineering, Heinz Nixdorf Institute, University of Paderborn, 33102 Paderborn, Germany `tobias.hesse@hni.uni-paderborn.de`

T. Sattel is with Faculty of Mechanical Engineering, Heinz Nixdorf Institute, University of Paderborn, 33102 Paderborn, Germany `sattel@hni.uni-paderborn.de`

1-4244-1068-1/07/$25.00 ©2007 IEEE.

The environment, that is the road borders and obstacles, is represented by a potential field hazard map, further also called external potential V^{ext}. An example of such a hazard map for a straight road with two static obstacles is shown in Fig. 2. A high potential signifies a high potential hazard, a low potential a low hazard.

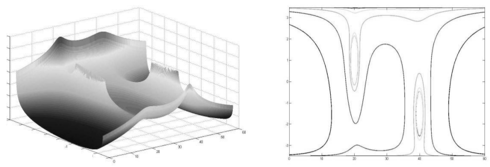

Fig. 2. Example of potential field hazard map (right: contour plot)

The external potential results as the sum of individual potential for the right and left border of the road, $V_i^{\mathrm{B}_r}$ and $V_i^{\mathrm{B}_l}$, and all obstacles O_j, $V_i^{\mathrm{O}_j}$

$$V^{\mathrm{ext}}\left(\mathbf{r}^{P_i},\ \mathbf{r}^{\mathrm{B}_r},\ \mathbf{r}^{\mathrm{B}_l},\ \mathbf{r}^{\mathrm{O}_j}, t\right) = V^{\mathrm{B}_l}\left(\mathbf{r}^{P_i},\ \mathbf{r}^{\mathrm{B}_l}\right) + V^{\mathrm{B}_r}\left(\mathbf{r}^{P_i},\ \mathbf{r}^{\mathrm{B}_r}\right) + \sum_{j=1}^{j_{\max}} V^{\mathrm{O}_j}\left(\mathbf{r}^{P_i},\ \mathbf{r}^{\mathrm{O}_j}, t\right), \tag{1}$$

where $\mathbf{r}^{\mathrm{B}_r}$, $\mathbf{r}^{\mathrm{B}_l}$ denote the position vectors to the corresponding points on the right and left border of the road and $\mathbf{r}^{\mathrm{O}_j}$ the position vector of the relevant point on the obstacle O_j. The motion of the obstacles is extrapolated based on their dynamic state. For more details refer to [10].

All external potentials are defined logarithmically:

$$\begin{aligned} V^{\mathrm{B}_r}\left(\mathbf{r}^{P_i},\ \mathbf{r}^{\mathrm{B}_r}\right) &= -k^{\mathrm{B}_r} \cdot \ln\left(\|\ \mathbf{r}^{P_i} -\ \mathbf{r}^{\mathrm{B}_r}\|\right), & (2)\\ V^{\mathrm{B}_l}\left(\mathbf{r}^{P_i},\ \mathbf{r}^{\mathrm{B}_l}\right) &= -k^{\mathrm{B}_l} \cdot \ln\left(\|\ \mathbf{r}^{P_i} -\ \mathbf{r}^{\mathrm{B}_l}\|\right), & (3)\\ V^{O_j}\left(\mathbf{r}^{P_i},\ \mathbf{r}^{\mathrm{O}_j}\right) &= -k^{O_j} \cdot \ln\left(\|\ \mathbf{r}^{P_i} -\ \mathbf{r}^{\mathrm{O}_j}\|\right). & (4)\end{aligned}$$

The external potential "pushes" the elastic band away from hazards and guarantees a collision-free trajectory. The repelling force $\mathbf{F}_i^{\mathrm{ext}}$ on each node P_i caused by these external potentials is defined as the gradient of the potential

$$\mathbf{F}_i^{\mathrm{ext}} = -\nabla_{\mathbf{r}^{P_i}} V^{\mathrm{ext}}. \tag{5}$$

Besides the external potentials, there exist also internal potentials, the spring-potentials of those springs interlinking the individual nodes of the band. These potentials prevent the band from "diverging" and ensure a "smooth" path. The internal spring potential of the spring between the nodes P_{i-1} and P_i is defined as

$$V_i^{\mathrm{spring}}\left(\mathbf{r}^{P_i},\ \mathbf{r}^{P_{i-1}}\right) = \frac{1}{2}k^{\mathrm{spring}}\left(\|\ \mathbf{r}^{P_i},\ \mathbf{r}^{P_{i-1}}\| - l_0\right)^2, \tag{6}$$

where l_0 denotes the relaxed spring length. The total internal potential V^{int} results as the sum of all individual spring potentials

$$V^{\mathrm{int}} = \sum_{i=1}^{N} V_i^{\mathrm{spring}}. \tag{7}$$

The internal force caused by this potential is computed analogously to the external forces as the gradient of the potential

$$\mathbf{F}_i^{\mathrm{int}} = -\nabla_{\mathbf{r}^{P_i}} V^{\mathrm{int}}. \tag{8}$$

The solution to the motion planning problem, i.e. the planned path, is now defined as the equilibrium solution for the elastic band, where

$$\mathbf{F} = \sum_{i=0}^{N}\left(\mathbf{F}_i^{\mathrm{int}} +\ \mathbf{F}_i^{\mathrm{ext}}\right) = \mathbf{0} \tag{9}$$

for all P_i, with $i \in \{0, N\}$.

III. INVERSE VEHICLE DYMANICS

The goal of this section is to analyze the vehicle dynamics and to calculate the necessary inputs and all tire forces for the vehicle to follow a certain desired path. For this purpose, a linear single-track model is used.

A. Vehicle Model

In order to derive the inverse dynamics, a linear single-track vehicle model is used. Here, the two tires of one axle are collapsed to one single tire in front and one in back. The center of gravity CG is assumed to lie on the road surface. Therefore, roll and pitch degrees of freedom are removed. The model is displayed in Fig. 3 and 4. The forces and velocities are depicted in Fig. 3, the used reference frames are shown in Fig. 4.

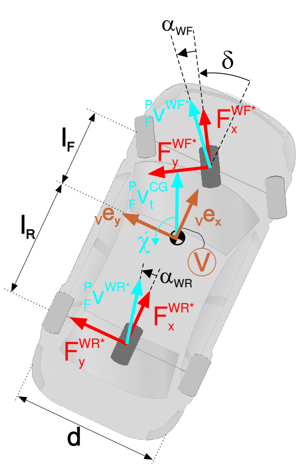

Fig. 3. Single-track model: forces and velocities

The planning-fixed reference frame P is an inertial reference frame and remains fixed during the path-planning. The vehicle-fixed reference frame V lies in CG with its x-axis pointing in longitudinal vehicle direction and the y-axis pointing to the left. In difference to V, F is rotated about the side-slip angle β, such that the vehicle's velocity with regards to P has the form

$${}^{P}\mathbf{v}^{CG} = {}^{P}_{V}v_x^{CG}\ {}_{V}\mathbf{e}_x + {}^{P}_{V}v_y^{CG}\ {}_{V}\mathbf{e}_y = {}^{P}_{F}v^{CG}\ {}_{F}\mathbf{e}_t. \tag{10}$$

The distances from CG to the front and rear axle are denoted l_F and l_R, respectively. The width of the car is given by d.

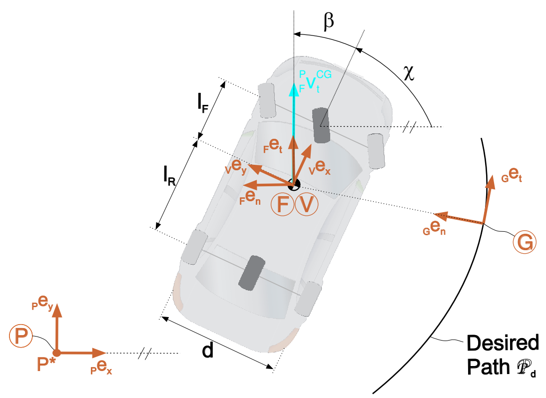

Fig. 4. Reference frames

Further, the steering angle δ and the slip angles α_{WF} and α_{WR} are indicated. The guidance reference frame G lies on the desired path $\mathcal{P}_d$ where the distance to the vehicle's center of gravity CG is minimal such that the ${}_G\mathbf{e}_n$-axis points towards CG. The resulting equations of motion read as

$$\underbrace{\begin{bmatrix} m_V & 0 & 0 \\ 0 & m_V & 0 \\ 0 & 0 & \Theta_z^{CG} \end{bmatrix} \begin{bmatrix} {}^P_V\dot{v}_x^{CG} \\ {}^P_V\dot{v}_y^{CG} \\ \ddot{\chi} \end{bmatrix}}_{\text{inertiaterms}} + \underbrace{\begin{bmatrix} -m_V\dot{\chi}\,{}^P_V v_y^{CG} \\ m_V\dot{\chi}\,{}^P_V v_x^{CG} \\ 0 \end{bmatrix}}_{\text{gyroscopic terms}} =$$

$$\underbrace{\overset{\text{selfdynamics}}{F_y^{WR*}\begin{bmatrix} 0 \\ 1 \\ -l_R \end{bmatrix}}}_{\text{non-controllable term}} + \underbrace{\overset{\text{steer and selfdynamics}}{F_y^{WF*}\begin{bmatrix} -\sin\delta \\ \cos\delta \\ l_F\cos\delta \end{bmatrix}}}_{\text{couplingterm}} + \underbrace{\overset{\text{brake, accelerate and steer}}{\begin{bmatrix} F_x^{WR*} + F_x^{WF*}\cos\delta \\ F_x^{WF*}\sin\delta \\ l_F\, F_x^{WF*}\sin\delta \end{bmatrix}}}_{\text{controllable term}}. \qquad (11)$$

The tires are modeled linearly, such that the lateral forces become

$$F_y^{\gamma*} = -C_\alpha^\gamma \alpha_\gamma,\ \gamma \in \{WF, WR\}, \qquad (12)$$

with the slip angles being

$$\alpha_{WF} = \arctan\left(\frac{{}^P_V v_y^{CG} + \dot{\chi} l_F}{{}^P_V v_x^{CG}}\right) - \delta, \qquad (13)$$

$$\alpha_{WR} = \arctan\left(\frac{{}^P_V v_y^{CG} - \dot{\chi} l_R}{{}^P_V v_x^{CG}}\right). \qquad (14)$$

B. Kinematics

After deriving the vehicle model that tells us how certain inputs influence the path of the vehicle, now the inverse way shall be taken to see what variables are given if a certain path is to be followed. The basic requirement is that the center of gravity CG moves on a given trajectory $\mathcal{P}_d$. For this case the reference frames F and G are identical. By a given trajectory, among others, the following inputs are given: The velocity of CG, ${}^P_F v_d^{CG}(s) = {}^P\mathbf{v}_t^{CG}(s)\ {}_F\mathbf{e}_t$, the desired acceleration of CG ${}^P_F\dot{\mathbf{v}}_d^{CG}(s)$, the desired curvature $\kappa_d^{CG}(s)$, and its derivative $\dot{\kappa}_d^{CG}(s)$. Based on this it is possible to give a relation between the angular velocity of the center of gravity CG of the vehicle and the curvature and velocity given by the trajectory,

$$\begin{aligned} {}^P_F v_d^{CG}\ {}_F\mathbf{e}_t &= -\left(\dot{\chi} + \dot{\beta}\right)\ {}_F\mathbf{e}_z \times R_{CG}\ {}_F\mathbf{e}_n \\ &= \left(\dot{\chi} + \dot{\beta}\right) \frac{1}{\kappa_d^{CG}}\ {}_F\mathbf{e}_t. \end{aligned} \qquad (15)$$

Reformulating 15 leads to

$$\left(\dot{\chi} + \dot{\beta}\right) = {}^P_F v_d^{CG}\ \kappa_d^{CG}. \qquad (16)$$

The derivative of 16 reads

$$\left(\ddot{\chi} + \ddot{\beta}\right) = \left({}^P_F\dot{v}_d^{CG}\ \kappa^{CG} + {}^P_F v_d^{CG}\ \dot{\kappa}^{CG}\right). \qquad (17)$$

Equation 16 and 17 can now be used to eliminate $\dot{\chi}$ and $\ddot{\chi}$ from 11 (3 equations) and 13 and 14, to be substituted in 12 (2 equations).

C. Necessary Inputs and Tire Forces

Now there are four known variables in five equations to account for eight unknown variables:

$${}^P_F v_d^{CG},\ {}^P_F\dot{v}_d^{CG},\ \kappa_d^{CG},\ \dot{\kappa}_d^{CG} \Rightarrow \beta, \dot{\beta}, \ddot{\beta}, \delta,\ F_x^{WF*},\ F_x^{WR*},\ F_y^{WF*},\ F_y^{WR*}.$$

Therefore, further simplifications are necessary. In order to reduce the number of unknowns, steady-state cornering with a constant velocity is assumed. Thus, $\dot{\beta}$ and $\ddot{\beta}$ are zero and are henceforth eliminated, leaving six unknown and two known variables:

$${}^P_F v_d^{CG},\ \kappa_d^{CG} \Rightarrow \beta, \delta,\ F_x^{WF*},\ F_x^{WR*},\ F_y^{WF*},\ F_y^{WR*}.$$

The equations are linearized for small angles β and δ. In addition, a relation between the longitudinal forces at the front and rear axle is introduced as sixth equation, rendering six equation for an equal number of unknown and two known variables

$$\begin{aligned} -m_V\ {}^P_F v_d^{CG2}\ \kappa_d^{CG}\beta &= C_\alpha^F\left(\beta + \kappa_d^{CG} l_F - \delta\right)\delta + \\ &\quad F_x^{WR*} + F_x^{WF*}, && (18) \\ m_V\ {}^P_F v_d^{CG2}\ \kappa_d^{CG} &= -C_\alpha^R\left(\beta - \kappa_d^{CG} l_R\right) + \\ &\quad \delta\ F_x^{WF*} - \\ &\quad C_\alpha^F\left(\beta + \kappa_d^{CG} l_F - \delta\right), && (19) \\ 0 &= l_R\, C_\alpha^R\left(\beta - \kappa_d^{CG} l_R\right) + \\ &\quad l_F\delta\ F_x^{WF*} - \\ &\quad l_F\, C_\alpha^F\left(\beta + \kappa_d^{CG} l_F - \delta\right), && (20) \\ F_y^{WF*} &= -C_\alpha^F\left(\beta + \kappa_d^{CG} l_F - \delta\right), && (21) \\ F_y^{WR*} &= -C_\alpha^R\left(\beta - \kappa_d^{CG} l_R\right), && (22) \\ F_x^{WR*} &= a\ F_x^{WF*}. && (23) \end{aligned}$$

The distribution a of longitudinal forces between the front and rear axle posted in 23 can be chosen arbitrarily with

$a \geq 0$. For a four-wheel driven vehicle it could be chosen $a \approx 1$.

Solving 18 to 23 for the steering angle δ, the side-slip angle β and the tire-forces $\mathbf{F}_{x,y}^{\gamma *}$ results in

$$\beta = \left(l_R - \frac{l_F\, m_V}{C_\alpha^R\,(l_F + l_R)}\, {}_F^P v_d^{CG\,2} \right) \kappa_d^{CG} \tag{24}$$

$$\delta = \left((l_F + l_R) + \frac{(\,C_\alpha^R l_R - C_\alpha^F l_F)\; m_V}{C_\alpha^F\, C_\alpha^R\,(l_F + l_R)}\, {}_F^P v_d^{CG\,2} \right) \kappa_d^{CG} \tag{25}$$

$$F_x^{WF*} = \frac{1}{(1+a)} \frac{\left(\,C_\alpha^F l_F^{\,2} + C_\alpha^R l_R^{\,2}\right) m_V^{\,2}}{C_\alpha^F\, C_\alpha^R\,(l_F + l_R)^2}\, {}_F^P v_d^{CG\,4}\, \kappa_d^{CG\,2} \tag{26}$$

$$F_x^{WR*} = \frac{a}{(1+a)} \frac{\left(\,C_\alpha^F l_F^{\,2} + C_\alpha^R l_R^{\,2}\right) m_V^{\,2}}{C_\alpha^F\, C_\alpha^R\,(l_F + l_R)^2}\, {}_F^P v_d^{CG\,4}\, \kappa_d^{CG\,2} \tag{27}$$

$$F_y^{WF*} = \frac{l_R m_V}{(l_F + l_F)}\, {}_F^P v_d^{CG\,2} \kappa_d^{CG} \tag{28}$$

$$F_y^{Wr*} = \frac{l_F m_V}{(l_F + l_F)}\, {}_F^P v_d^{CG\,2} \kappa_d^{CG}. \tag{29}$$

IV. INTERPOLATION OF PATH

In the previous section, the path was assumed to be given in a continuous form. For the motion planning with elastic bands, however, this is not the case. Here, the path is given by a number of discrete nodes. Therefore, the question arises how to determine the velocity and curvature from this discrete representation of the path. These quantities only have to be known at these nodes, not in between, since the additional potential V^{dyn} shall be defined only at each node.

The curvature at one node can be calculated from the radius of the circle that is defined by itself and its two adjacent nodes. This is illustrated in Fig. 5.

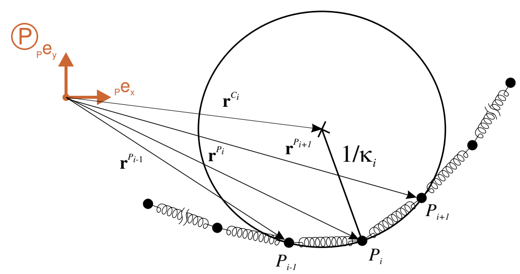

Fig. 5. Curvature approximation over 3 nodes

The general equation for the circle reads

$$(\,r_x - r_x^{C_i})^2 + (\,r_y - r_y^{C_i})^2 = R^2, \tag{30}$$

where R is the radius of the circle, $\mathbf{r}^{C_i}$ denotes the position vector to the center of the circle and $\mathbf{r}$ is any point on the circle. If now three nodes (P_{i-1}, P_i, P_{i+1}) are assumed to be on the circle, we have three equations for three unknowns (R, $\mathbf{r}_x^{C_i}$, $\mathbf{r}_y^{C_i}$). Thus we can solve for the curvature

$$\kappa_{d,P_i}^{CG} = \kappa_i = \frac{1}{\sqrt{\left(\,r_x^{P_i} - r_x^{C_i}\right)^2 + \left(\,r_y^{P_i} - r_y^{C_i}\right)^2}}. \tag{31}$$

The velocity-profile is given by the driver. Based on the current inputs to the brake and acceleration pedal, a constant acceleration (positive or negative) is assumed (up/down to a certain maximum or minimum velocity, of course). From this, the velocity along the arc length s can be calculated. Hence, the velocity at each node is known.

V. INTEGRATION OF VEHICLE DYNAMICS IN ELASTIC BAND PATH PLANNING

Based on the calculations above and the noted simplifications and assumptions, it is possible to determine all necessary dynamic quantities for the single-track model for a given trajectory to be followed. Further it has been demonstrated how to calculate parameters like curvature and velocity from a discrete representation of a path. These results shall now be used to integrate the vehicle dynamics in the motion planning such that the adhesion potentials at the tires are maximized and more drivable paths result. For this purpose, an additional internal potential for the method of elastic bands is defined. The idea bases upon Kamm's circle as picture for the adhesion limit at each tire, as depicted in Fig. 6.

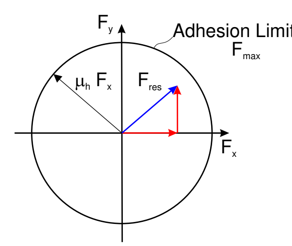

Fig. 6. Kamm's circle

According to Kamm, the adhesion limit is given by a radius of F_{max} which depends on the tire load F_z and the road-tire friction coefficient μ_h, as can also be seen in Fig. 6. Therefore, the total force F_{res} (geometric sum of x- and y-components) at each tire must be smaller than F_{max}, i.e. it must remain inside Kamm's circle

$$F_{\mathrm{res}}^{\gamma *} = \sqrt{F_x^{\gamma *\,2} + F_y^{\gamma *\,2}} \leq \mu_h\, F_z^{\gamma *} = F_{\mathrm{max}}^{\gamma *}, \quad \gamma \in \{WF, WR\}\,. \tag{32}$$

The tire loads at front and rear tire result from a static equilibrium (since CG is assumed to be on the road surface and no pitch degree of freedom exists). They are given by

$$F_z^{WF*} = \frac{l_R}{(l_F + l_R)} m_V\, g \tag{33}$$

and

$$F_z^{WR*} = \frac{l_F}{(l_F + l_R)} m_V\, g, \tag{34}$$

where m_v denotes the vehicle's mass and g the gravitation. At this point we can already evaluate a planned path with a given velocity profile with regards to its drivability by calculating the necessary forces and comparing them with the maximum forces from Kamm's circle.

The next step is to enhance the motion planning itself in order to achieve more drivable paths by introducing an additional internal potential. The new internal dynamics potential V^{dyn} shall be defined based on the ratio of the necessary total force at each axle and the possible maximum force. At each node P_i it is defined as

$$\begin{aligned} V_i^{\text{dyn}} &= k^{\text{dyn}} \left[\left(\frac{F^{WF*}_{\text{res},i}}{F^{WF*}_{\text{max},i}} \right)^n + \left(\frac{F^{WR*}_{\text{res}},i}{F^{WR*}_{\text{max},i}} \right)^n \right] \\ &= k^{\text{dyn}} \left(\frac{\sqrt{F^{WF*2}_{x,i} + F^{WF*2}_{y,i}}}{F^{WF*}_{\text{max},i}} \right)^n + \\ & \quad k^{\text{dyn}} \left(\frac{\sqrt{F^{WR*2}_{x,i} + F^{WR*2}_{y,i}}}{F^{WR*}_{\text{max},i}} \right)^n . \end{aligned} \tag{35}$$

This potential is illustrated in Fig. 7.

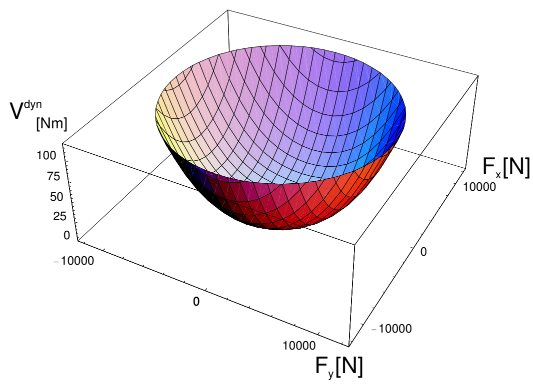

Fig. 7. Internal vehicle dynamics potential

Therefore, the total dynamics potential results as the sum of the potentials at all nodes P_i

$$V^{\text{dyn}} = \sum_{i=0}^{N} V_i^{\text{dyn}}, \tag{36}$$

and the resulting dynamics force $_{P}\mathbf{F}_i^{\text{dyn}}$ that excites the elastic band at the node P_i is defined analogously to the other potentials of the method of elastic bands as the gradient of the total dynamics potential

$$\mathbf{F}_i^{\text{dyn}} = -\nabla_{\mathbf{r}^{P_i}} V^{\text{dyn}}. \tag{37}$$

In order to integrate this newly defined potential into the method of elastic bands, only 7 has to be redefined to

$$V^{\text{int}} := \sum_{i=1}^{N} V_i^{\text{spring}} + \sum_{i=0}^{N} V_i^{\text{dyn}}. \tag{38}$$

The rest of the procedure to calculate collision-free and drivable trajectories remains unaltered.

VI. RESULTS

The presented improvement has been implemented in the method of elastic bands. The results for the path-planning are shown for an example scenario with a straight, two-lane road and one static obstacle about 50 meters in front of the

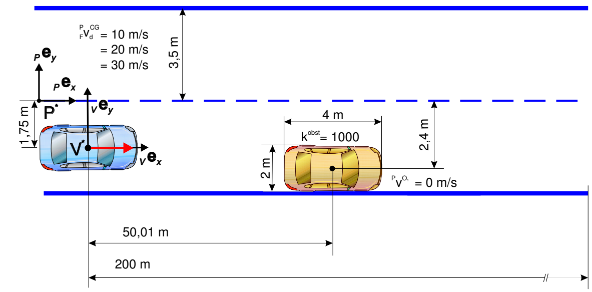

Fig. 8. Example scenario with one static obstacle

host vehicle, as illustrated in Fig. 8. The trajectory is planned for different constant velocities, $10\frac{m}{s}$, $20\frac{m}{s}$, and $30\frac{m}{s}$.

For this example scenario the method of elastic bands is used first without and then including the new internal dynamics potential. Fig. 9 shows the resulting path(s) without V^{dyn}. As can be seen, the path is always the same and does not depend on the velocity of the host vehicle.

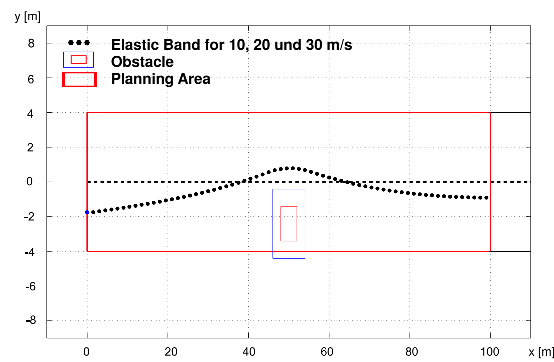

Fig. 9. Elastic band without new potential for different velocities

Based on 26 to 29, the necessary tire-forces can now be calculated for this planned path. This is shown in Fig. 10. The figure also indicates the maximum total tire force for the front and rear tire of the single-track model according to Kamm's circle. The resulting curves are not very smooth, since they consist of discrete values only for each node of the elastic band.

It can be seen that the necessary force exceeds the maximum for higher velocities. This indicates, that the path is not drivable as it is planned. The exceedingly high necessary forces occur mainly around the position of the obstacle. In addition, a short high peak can be seen at the very beginning. This peak is due to the fact that the first two nodes are fixed during the path-planning which results in a sharp bend at the second node. Without further modifications this cannot be prevented.

When introducing the newly defined internal dynamics potential, the planned paths result as shown in Fig. 11. The most obvious difference is that now the paths depends on the vehicle's velocity. The faster the host vehicle, the lower the curvature of the planned path. This can be seen more precisely in Fig. 12, where again the curvature and tire forces are shown for the planned paths.

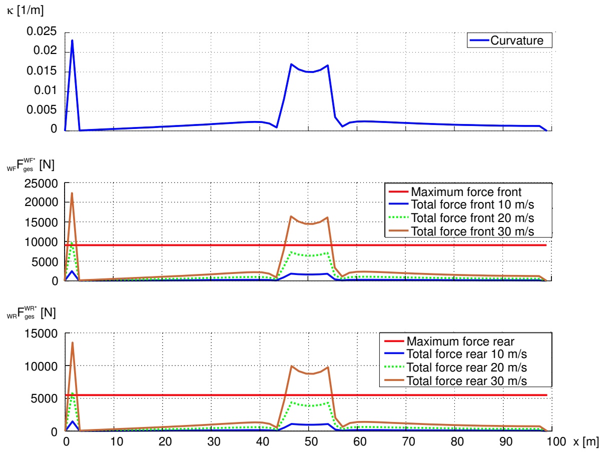

Fig. 10. Curvature and forces without new potential for different velocities

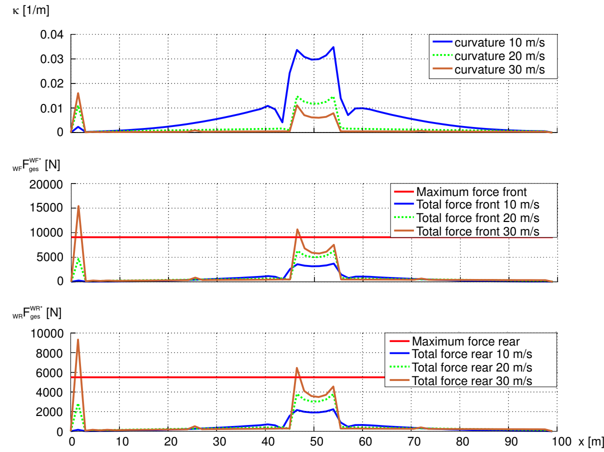

Fig. 12. Curvature and forces with new potential for different velocities

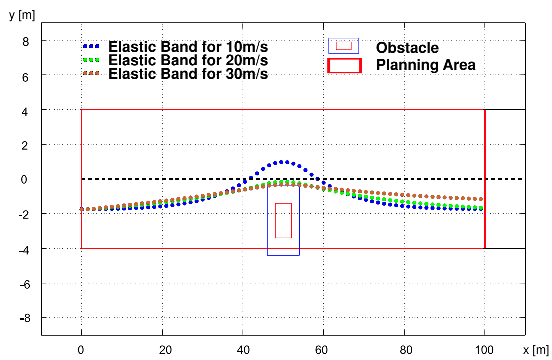

Fig. 11. Elastic band with new potential for different velocities

It can be seen that the necessary forces around the obstacle have been reduced, creating a more drivable path.

VII. CONCLUSIONS AND FUTURE WORKS

Now it is possible to estimate the drivability of a certain path that is given either in continuous form or as a set of discrete points. Further a method has been shown to integrate the vehicle dynamics into the motion planning with elastic bands and therefore enhance the drivability of the planned paths. Thus, the mentioned disadvantage that the method of elastic bands had until this point has been greatly reduced. Due to some assumptions that had to be made along the way (road-tire friction coefficient, tire-loads, single-track model, stationarity, constant velocity) this method is not exact. However, it can provide a good first estimate to reject paths that do not seem to be drivable at all or to enhance the planned motion within the planning method.

For the future, enhancements are planned to overcome the initial peak-curvature and to study the effects this new potential has when included in the overall assistance system. Further, the equilibrium position of the elastic band is given by a system of nonlinear equations (9). The solution of this equation requires an iterative numerical procedure. Unfortunately, the introduction of the new dynamics potential has increased the number of necessary iterations. Therefore, future efforts also have to aim at a reduction of the number of iterations and calculation time to reach a real-time capability.

REFERENCES

[1] Claus Brüdigam (1994), *Intelligente Fahrmanöver sehender autonomer Fahrzeuge in autobahnähnlicher Umgebung*, PhD-Thesis, University of the Federal Armed Forces, Muenich, Germany, (Translated title: Intelligent Maneuvers of autonomous ground vehicles with sensor-vision on highway-like environments)

[2] Reichardt, D. (1996), *Kontinuierliche Verhaltenssteuerung eines Autonomen Fahrzeugs in Dynamischer Umgebung*, PhD-Thesis, University of Technology Kaiserslautern, Germany, (Translated title: Continous behaviour based control of an autonomous ground vehicle in dynamic environment)

[3] Stiller, C.; Simon, A.; Weisser, H. (2001) *A driving robot for autonomous vehicles on extreme courses*, In: Proc. 1th Conference on Telematics Applications in Automation and Robotics. Ravensburg-Weingarten, July 2001, pp. 361-367

[4] Mildner, Frank, (2004) , *Untersuchungen zur Erkennung und Vermeidung von Unfällen für Kraftfahrzeuge*, PhD-Thesis, *Helmut Schmidt University, University of the Federal Armed Forces*, Hamburg, Germany, (Translated title: Investigations of the detection and avoidance of accidents for vehicles)

[5] Monemerlo, Michael; Thrun, Sebastian; Dahlkamp, Hendrik; Stavens, David; Strohband, Sven (2006): *Winning the DARPA Grand Challenge with an AI Robot*, The 21th National Conference on Artificial Intelligence and the 18th Innovative Applications of Artificial Intelligence Conference, AAAI, July 16-20, 2006, Boston, Massachusetts, USA

[6] Krogh, B. H. (1984) *A Generalized Potential Field Approach To Obstacle Avoidance Control*, In Proceedings Of International Robotics Research Conference Bethlehem, Pennsylvania, August 1984

[7] Khatib, O. (1986) *Real-time obstacle avoidance for manipulation and mobile robots*, International Journal of Robotics Research, 5(1):9098, 1986.

[8] Latombe, J.-C. (1993) *Robot motion planning*, Kluwer Academic Publisher, ISBN 0-7923-9206-X

[9] Sattel, T. and Brandt, T. (2005) *Ground Vehicle Guidance along Collision-Free Trajectories using Elastic Bands*, 2005 American Control Conference (ACC), Portland, Oregon, USA, June 10, IEEE Catalog Number: 05CH37668C, ISBN: 0-7803-9099-7, pp. 4991-4996

[10] Brandt, Thorsten; Sattel, Thomas; Wallaschek, Jörg, (2006), *Towards vehicle trajectory planning for collision avoidance based on elastic bands*, Int. J. of Vehicle Autonomous Systems, forthcoming